Research Paper

Haloform formation in coastal wetlands along a salinity gradient at South Carolina, United States

Jun-Jian Wang,[A] *Yi Jiao,*[B] *Robert C. Rhew*[B] *and Alex T. Chow*[A,C]

[A]Baruch Institute of Coastal Ecology and Forest Science, Clemson University,
 PO Box 596, Georgetown, SC 29442, USA.
[B]Department of Geography and Berkeley Atmospheric Sciences Center,
 University of California at Berkeley, Berkeley, CA 94720, USA.
[C]Corresponding author. Email: achow@clemson.edu

Environmental context. Natural haloform emissions contribute to stratospheric ozone depletion but there are major unknown or underestimated sources of these gases. This study demonstrates that soil and water at tidal wetlands are important haloform sources, and emissions peak at the forest–marsh transition zone. The low-lying forested wetlands of the south-eastern United States that are facing sea-level rise and seawater intrusion may become hotspots for haloform emission.

Abstract. Soil haloform emissions are sources of reactive halogens that catalytically deplete ozone in the stratosphere but there are still unknown or underestimated haloform sources. The >200 000 ha of low-lying tidal freshwater swamps (forests and marshes) in the south-eastern United States could be haloform (CHX_3, X = Cl or Br) sources because sea-level rise and saltwater intrusion bring halides inland where they mix with terrestrial humic substances. To evaluate the spatial variation along the common forest–marsh salinity gradient (freshwater wetland, oligohaline wetland and mesohaline saltmarsh), we measured chloroform emissions from in situ chambers and from laboratory incubations of soil and water samples collected from Winyah Bay, South Carolina. The in situ and soil-core haloform emissions were both highest in the oligohaline wetland, whereas the aqueous production was highest in mesohaline saltmarsh. The predominant source shifted from sediment emission to water emission from freshwater wetland to mesohaline saltmarsh. Spreading out soil samples increased soil haloform emission, suggesting that soil pores can trap high amounts of $CHCl_3$. Soil sterilisation did not suppress $CHCl_3$ emission, indicating the important contribution of abiotic soil $CHCl_3$ formation. Surface wetland water samples from eight locations along a salinity gradient with different management practices (natural *v.* managed) were subjected to radical-based halogenation by Fenton-like reagents. Halide availability, organic matter source, temperature and light irradiation were all found to affect the radical-based abiotic haloform formation from surface water. This study clearly indicates that soil and water from the studied coastal wetlands are both haloform sources, which however appear to have different formation mechanisms.

Additional keywords: bromide, chloroform, dissolved organic matter, ozone depletion, salinity, Winyah Bay.

Received 1 November 2014, accepted 1 December 2015, published online 29 February 2016

Introduction

Haloforms (CHX_3; also known as trihalomethanes) are sources of reactive halogens (X = Br, Cl, I) to the troposphere and lower stratosphere, contributing to the atmospheric budget of very-short-lived substances and to catalytic ozone depletion in the stratosphere.[1–3] In the water industry, haloforms have also been of great interest to water engineers since the 1970s[4] because of their potential carcinogenic risks and non-carcinogenic toxicity to human beings as disinfection byproducts.[5,6] Water disinfection and pulp bleaching are well-known anthropogenic sources of haloform, but account for a decreasing fraction of haloform emissions because pulp manufacturing has largely switched bleaching methods.[7–9] More than 90 % of chloroform and 70 % of bromoform globally are estimated to originate from natural sources,[7,10] with soil processes and seawater emission as prominent sources respectively.[11] Natural sources identified

since the 1990s are widespread in global terrestrial ecosystems.[12–18] Known methods of haloform production include haloperoxidase-mediated and Fenton or Fenton-like radical-based halogenation of natural organic matter, as well as natural thermal processes (fires, volcanoes and hydrothermal processes).[11,15,19–22]

Separating abiotic and biotic processes in soil and water requires a mechanistic understanding of production and knowledge of associated intermediate compounds. An abiotic route to formation of halocarbons such as chloroacetic acid and chloroform has been shown by Fenton-like reactions acting on phenolic moieties such as ethoxyphenol and catechol, which are considered model substances of monomeric units of humic acids.[19,23,24] A biotic route to haloform formation is mainly associated with litter-decomposing organisms (e.g. bacteria, fungi and termites) that can produce enzymes (e.g. haloperoxidases and halogenases)

converting inorganic halogens to organohalogens.[25–28] The yields and speciation of halocarbons have been suggested to be associated with the degree of humification and sources of natural organic matter.[20,29–33] In either abiotic or biotic processes, formation of reactive halogen species such as hypochlorous acid or hypobromous acid with reactive oxygen species (ROSs) is considered as one of the pathways in halogenation processes.[23,34,35]

Rising sea level (up to 9.1 mm year^{-1} on the Louisiana coast) along the flat south-eastern US coastal plain could significantly change both vegetation composition and salinity of coastal ecosystems.[36] Conservative estimates indicate more than 200 000 ha of tidal freshwater swamps, including forested wetlands and marshes, along the coast of the south-eastern US, and South Carolina has the largest distribution with over 60 000 ha.[37,38] As the boundary between the low-lying coastal forest and high marsh moves upslope owing to sea-level rise, the plant composition, primary productivity, biogeochemical cycles and even the function of the freshwater wetlands can be considerably different from their previously unaltered states.[38–40] Forest vegetation (e.g. *Pinus*, *Quercus* and *Vaccinium*) is successively replaced by coastal salt marsh (e.g. *Juncus* and *Spartina*).[41,42] Sodium and chloride become the dominant cation and anion respectively in seawater inundation areas. Opening of the forest canopy due to dieback allows greater sunlight penetration, which may promote photochemical halogenation reactions in surface water.[35,43] Also, seawater intrusion may bring in halogenating enzymes from marine organisms in coastal environments.[27] The production of hydrogen peroxide (H_2O_2), singlet oxygen ($^1O_2$), hydroxyl radical ($^{\bullet}OH$) and other reactive species by photo-Fenton reactions, resulting in photobleaching of coloured dissolved organic matter (DOM), has been observed in coastal rivers and seawaters.[44–46] Particularly, high levels of organic carbon are common in waters (up to 50 mg L^{-1}) of the tidal freshwater forest wetlands, which may serve as source materials for haloform formation.[47] Therefore, the prerequisites for haloform formation in coastal wetlands in the south-eastern US are likely satisfied, but information about halocarbon biogeochemistry in this region is very limited.

To understand how sea-level rise or seawater intrusion may affect the haloform emissions, the present study measured the haloform emissions from in situ field chambers along a salinity gradient (freshwater wetland → oligohaline wetland → mesohaline saltmarsh) in Winyah Bay, South Carolina, USA. By comparing the soil emission and aqueous production, we aimed to explore whether soil emission is the dominant source for all sites. In the laboratory soil incubation, effects of soil porosity and enzymatic process on soil haloform emission were evaluated by limiting soil pores by spreading the material out and microbial activity by thermal sterilisation respectively. In the laboratory water incubation, Fenton-like reagents were added to natural water samples to test the possibility of radical-based haloform formation from water and the effects of halide availability, DOM source, temperature and sunlight. The current study focussed on the chlorinated and brominated haloforms owing to their expected higher abundance over iodinated species.

Materials and methods

Study sites

Four natural and two managed wetlands in Winyah Bay, South Carolina, USA, were included in the present study. Winyah Bay (33°16′29″N, 79°14′43″W) is the estuary associated with the third-largest watershed draining into the Atlantic Ocean on the east coast of the USA (Fig. 1). These blackwater-dominated, low-lying wetland ecosystems have experienced severe salt-water intrusion, converting freshwater forested wetland to degraded oligohaline wetland and to salt marsh.[40,48]

A forest–marsh transect was chosen to cover four natural wetlands within Hobcaw Barony in North Winyah Bay: freshwater wetland (Site 1), oligohaline wetland (Site 2), mesohaline saltmarsh (Site 3) and euhaline saltmarsh (site 4). The 2.4-ha freshwater wetland (Site 1) is a healthy forested wetland with a water salinity of 0.5 ppt or less and dominated by bald cypress (*Taxodium distictum*), water tupelo (*Nyssa aquatica*) and swamp tupelo (*Nyssa sylvatica* var. *biflora*).[49] The oligohaline wetland (Site 2) is a salt-affected forested wetland and has experienced moderate saltwater intrusion, with a salinity of 0.5–5 ppt. Some species progressively fall out of the vegetation assemblage as the canopy opens, leaving only bald cypress and a scattering of swamp tupelo. The mesohaline saltmarsh (Site 3) is defined as having originally been freshwater wetland that now receives saline water inputs, resulting in a salinity of 18 ppt or less. All hardwood species have died and been replaced with salt marsh vegetation (e.g. *Juncus* and *Spartina*).[39] Stumps are still visible but are progressively covered by sediment accretion. The euhaline saltmarsh (Site 4) is located in the North Inlet of Winyah Bay with a single outlet to the sea and three major tidal creeks. The marsh creeks have a mean tide range of 1.7 m and recorded peak current velocities of 2.3 m s^{-1}. The marsh is strongly influenced by oceanic water and the salinity seldom falls below 32 ppt. The dominant flora is the cordgrass *Spartina alterniflora*. Site 1 is considered an isolated freshwater wetland, whereas Sites 2, 3 and 4 are considered tidal wetlands. Details of wetlands in this transect have been described elsewhere.[47,48]

In contrast to North Winyah Bay, flood control gates are in place for water and wetland management in Yawkey Wildlife Center in South Winyah Bay. A managed freshwater and a managed saltwater wetland from the Yawkey Wildlife Center were also selected for the study. The freshwater wetland has a surface area of ∼125 ha with an average water depth of ∼0.5 m. Waters were collected from the inflow (Site 5) and outflow (Site 6). The managed saltwater wetland has an area of 20 ha with an average water depth also ∼0.5 m. The area was generally flooded in the duck-hunting season (Oct–April) but is completely drained during the summer. Water samples were also collected from the inflow (Site 7) and the outflow (Site 8).

In situ field flux measurements

We conducted in situ field flux measurements at the freshwater forested wetland (Site 1), oligohaline forest wetland (Site 2) and mesohaline saltmarsh (Site 3) on 14–17 May 2012, using the static chamber method.[50,51] At each site, four chamber experiments were conducted, with a pair of large aluminium chambers (53.7 × 53.7 × 44.1-cm lid and 51.4 × 51.4 × 22.9-cm base) and a pair of smaller polycarbonate chambers (29.4 × 29.4 × 30.5-cm lid and 29.4 × 29.4 × 30.5-cm base). The aluminium chamber bases were installed the day before the field measurements whereas the polycarbonate chambers were installed 6 months prior. The freshwater forested wetland sites were entirely inundated, with no vegetation above water level within the chambers. The oligohaline forest wetland sites were all muddy with little to no aboveground vegetation, although one aluminium chamber site contained a cypress knee inside the footprint of the chamber. The mesohaline saltmarsh sites all
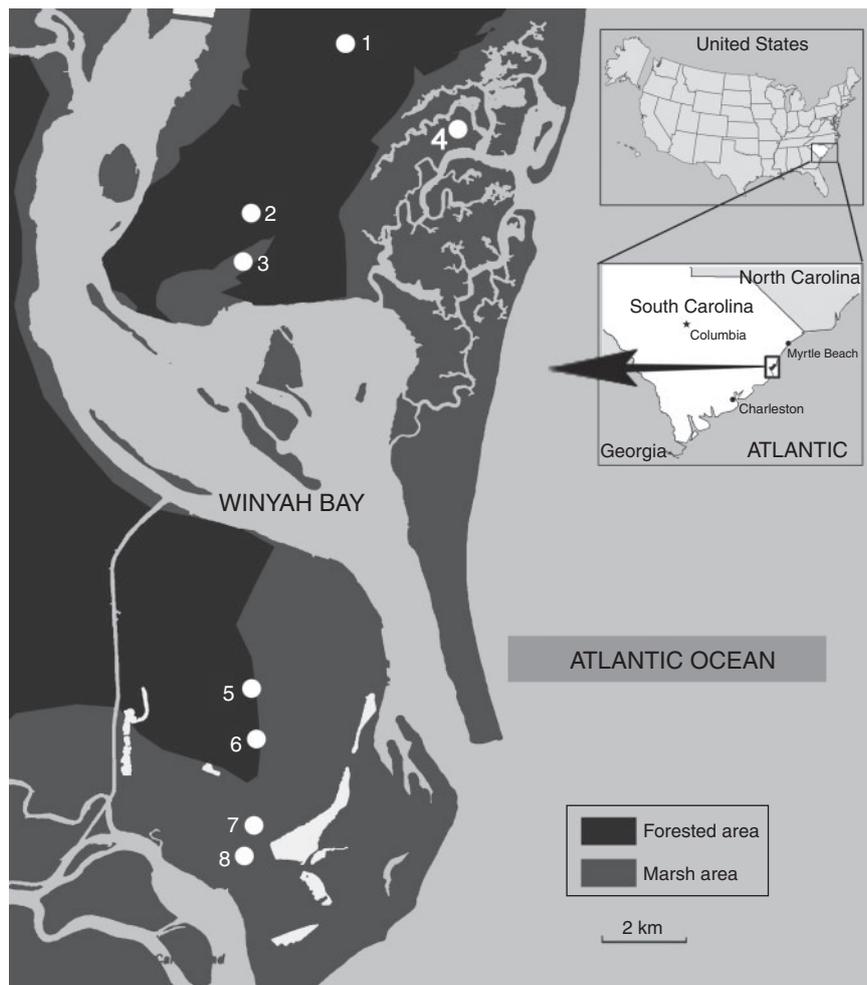
Fig. 1. Sampling locations in South and North Winyah Bay, South Carolina: freshwater wetland (1); oligohaline wetland (2); mesohaline saltmarsh (3); euhaline saltmarsh (4); inflow (5), and outflow (6) of managed freshwater wetland; and inflow (7), and outflow (8) of managed saltwater wetland.

were inundated with salt water but with dense emergent *Spartina* cordgrass contained within the footprint of the chamber.

Briefly, gas samples were collected from the chamber headspace at the beginning and end of the chamber closing (at 1 and 20 min). Air samples were collected in previously evacuated canisters (1-L electropolished stainless steel or 3-L silica-lined stainless steel) for haloform analysis by gas chromatography–mass spectrometry (GC-MS; Agilent 6890N/5973, Agilent Technologies, Santa Clara, CA) (see below). The air temperatures inside and outside the chamber were recorded using iButtons (Dallas Semiconductor Maxim, Sunnyvale, CA). Each air sample was measured 2 to 4 times by GC-MS (see below), and each concentration measurement was plotted against time of enclosure. The net flux was calculated as the net increase of moles of trace gases in the chamber (concentration × volume) divided by the basal area of the chamber and chamber enclosure time and expressed in units of nanomoles per square metre per day. The error in the slope of the linear regression (95 % confidence interval) was propagated with the error in the number of moles of air in the chamber to derive the flux error.

The two types of chambers did not show significantly different $CHCl_3$ fluxes overall ($P = 0.25$), but the polycarbonate chambers did show an internal temperature increase (averaging

4 °C higher relative to outside chamber temperatures), in contrast to the aluminium chambers (averaging 1 °C lower), consistent with partial sunlight penetration in the translucent polycarbonate chambers. Using two-point concentration trends may underestimate the flux if gas-phase enrichment is non-linear (i.e. a function of chamber concentration), but in other studies using three time points, the concentration trends were linear over this time period of enclosure (e.g. Khan et al.[51,52]).

Controlled laboratory incubation

Soil core incubations

Twelve surface-soil samples (0–5 cm) were collected between 14 January and 17 March 2015, four each from three different sites (freshwater wetland, oligohaline wetland and mesohaline saltmarsh). Soil cores were collected into aluminium sheaths using a soil corer (AMS Inc., American Falls, ID), shipped to the University of California at Berkeley and stored at ~5 °C until analysis. Prior to each set of incubation experiments, soil samples sat at room temperature for at least 12 h. For each incubation, the soil sample was sealed in a glass Mason jar (1.9 L) so that exchanged gases could be observed through the changing composition of the headspace. Right before the start of each incubation, the headspace was flushed with ambient air for ~30 s. The

jar was then sealed with a Viton O-ring and a stainless-steel lid. Headspace samples were drawn from the incubation jar three times at intervals of 40 min into a previously evacuated stainless-steel loop (~25 mL) that was connected to the preconcentration system of the GC-MS.

Each soil core was incubated twice consecutively on the same day. It was noted that the first $CHCl_3$ incubation generally had higher emissions than the second incubation, probably owing to the release of previously formed $CHCl_3$ trapped in the soil pores. Therefore, two of the four samples were removed from the sheath and spread out on the bottom of the Mason jar (increasing the exposed surface area by 2.48 times and reducing the soil porosity), and the emissions were measured twice to explore the effects of altered exposed area and soil porosity on $CHCl_3$ emissions. Subsequently, all soil samples were steam-sterilised by heating in an oven at 85–90 °C while covered for 1 h.[53] To minimise the potential thermogenic $CHCl_3$, sterilised soils were cooled down for 24 h, which allowed $CHCl_3$ emission before the incubation experiments in the same way as for live soils. To keep the soil moisture constant during storage and measurement, deionised water was added into the samples based on the differences of weight measured after collection and 24 h before each measurement. The net flux was calculated in the same way as for the flux chambers, except divided by the surface area of the exposed soil core (17.8 cm^2 for intact cores). For comparison purposes, flux calculations for the spread out soils (~44 cm^2) used the same surface area as intact cores.

Gas samples were analysed at the University of California, Berkeley, using an Agilent 6890N/5973 quadrupole GC-MS.[12,51] Air canisters were analysed within 3 weeks of sample collection, and soil cores were incubated 0.5 to 4 weeks after collection. During the measurements, several calibration curves were constructed using whole-air standards collected at Trinidad Head, CA, or Niwot Ridge, CO, and calibrated at the Scripps Institution of Oceanography and the National Oceanographic and Atmospheric Administration (NOAA) Global Monitoring Division Laboratory respectively. All gas concentrations are reported in the units of dry air mole fractions (ppt, 10^{-12} mol mol^{-1}). Bromoform was monitored in air samples but was not quantified, owing to the lack of a suitable gas standard and incomplete assessment of detection limits and potential loss in the sampling system. Most samples were below the detection limit of the instrument. Thus, only qualitative remarks about the largest bromoform peaks can be reported.

Water collection and characterisation

Grab water samples were collected using 500-mL amber glass bottles within 3 h of high tide on 20 May 2012. Bottles were completely filled without headspace, stored in an ice cooler and transferred back to the Baruch Institute laboratory in Georgetown, South Carolina. For the natural wetland samples in North Winyah Bay, three bottles of water were collected randomly from different locations within the site as replicates. Water samples were then filtered through a 0.45-μm polyether-sulfone membrane (Supor-450, Pall Corporation, Ann Arbor, MI) and stored at 4 °C before analyses.

All filtered water samples were measured for pH and electrical conductivity at temperature 25 °C (EC_{25}) using an Accumet XL60 dual channel meter (Fisher Scientific, Pandan Crescent, Singapore). Concentrations of dissolved organic carbon (DOC) and total dissolved nitrogen (TDN) were analysed using a TOC/TN analyser (Model TOC-Vcsh, Shimadzu, Kyoto, Japan). Concentrations of inorganic nitrogen (NH_4^+–N

and NO_x^-–N) and PO_4^{3-}–P were determined using a Systea Easychem discrete analyser (Systea Scientific, Oak Brook, IL).[47] Anions including chloride, bromide and sulfate were determined using ion chromatography (IC, Metrohm, Riverview, FL) with a Metrosep ASUPP7–250 column.[54,55] The absorbance of each water sample was scanned from 200 to 700 nm using a UV-1800 UV-Vis spectrometer (Shimadzu, Kyoto, Japan), and specific ultraviolet absorbance (SUVA) was calculated by normalising ultraviolet absorbance at 254 nm to DOC concentration (L mg^{-1} m^{-1}). SUVA has been widely used as a surrogate of aromatic carbon content of DOC.[56] In addition, we also calculated the E2/E3 ratio (i.e. UV absorbance at 254 nm divided by absorbance at 365 nm), which is an important index of molecular size[57] and photoreactivity of DOC.[58]

The three-dimensional excitation–emission-matrix fluorescent scans (excitation (Ex) range: 220–450 nm; emission (Em) range: 220–550 nm) for water samples were conducted in an RF5301 spectrofluorometer (Shimadzu) with Ex and Em slit widths of 5 nm. Scanned fluorescence excitation–emission matrices (EEM) were corrected[59] to remove the instrument-dependent effects, inner-filter effects and Raman effects, and to standardise the units to Raman units (normalised to the integral of the Raman signal between 390 and 410 nm in emission at a fixed excitation of 350 nm). To account for reabsorption of the light emitted by fluorophores in a concentrated water sample, all samples were diluted with Milli-Q water to an ultraviolet absorbance at 254 nm of 0.3 or less. Several indices based on fluorescence EEMs were calculated, including the fluorescence index (FI), humification index (HIX) and freshness index (β/α).[60] Briefly, the fluorescence index, an indicator for terrestrial origin (~1.3) or microbial origin (~1.8) of the DOM, was calculated as the fluorescent response of Em at 470 nm divided by that at 520 nm, at Ex 370 nm. The humification index, which is positively linked to the abundance of the humic substance and the degree of humification, was calculated as the fluorescent area under the 435–480-nm Em spectra divided by the 300–345-nm peak area, at Ex 254 nm. The freshness index (β/α), an indicator of the abundance of freshly produced autochthonous DOM, was calculated as the fluorescent ratio of Em intensity at 380 nm divided by the Em intensity maximum observed between 420 and 435 nm, at Ex 310 nm. The protein content and redox index were calculated from Cory and McKnight's PARAFAC model.[61] The redox index, ranging from 0 (oxidised) to 1 (reduced), is an index linked to the redox status of the quinone-like moieties of the DOM.

Water incubations and radical-based abiotic halogenation tests

Within 12 h of water sample collection, 10-mL unfiltered subsamples were transferred to two 20-mL screw-top clear headspace vials by glass pipette. One vial was immediately analysed for haloform occurrence using a headspace gas chromatograph–electron capture detector (GC-ECD; Agilent 7890, Agilent Technologies) and noted as the background haloform level. Another vial was incubated for 24 h at 25 °C in the laboratory and analysed for haloform levels. The calculated difference of haloform levels between the 24-h incubation sample and the background sample is the 24-h aqueous production of haloforms.

For the radical-based abiotic halogenation of water samples, 10 mL of filtered water sample was transferred to a 20-mL amber headspace vial. Then, 100 μmol H_2O_2 (from ~30 %

H_2O_2; Acros Organics, Morris Plains, NJ) and 100 μmol Fe^{3+} (in the form of $Fe_2(SO_4)_3$; Acros Organics) were carefully added to a gently shaking vial and capped quickly. The actual H_2O_2 concentration was determined by $KMnO_4$ titration each time immediately before addition to accurately quantify the initial amount of H_2O_2 in the vial. All headspace vials were incubated for 24 ± 0.5 h and analysed by GC-ECD. Blank and parallel tests were also conducted for quality control and quality assurance. Additions of 100 μmol H_2O_2 into the 10-mL of water samples without addition of Fe^{3+} (H_2O_2-only treatment) for the 24-h incubation were also tested. All glassware used in the present study was acid-washed (10 % HCl for 24 h), rinsed with deionised) water three times and baked at 200 °C for 4 h.

To quantify the effects of temperature and solar radiation on the 24-h haloform production, water samples of the mesohaline saltmarsh were subjected to four different treatments: (i) 4 °C in a dark environment, (ii) 25 °C in a dark environment, (iii) 40 °C in a dark environment, and (iv) 25 °C under light irradiation. For the irradiation treatment, clear headspace vials were used instead of amber headspace vials, and a sunlight simulator (Perfect Light, PLS-SXE300C, Beijing, China; 2000 mW cm^{-2}) was used (see Fig. S1 in Supplementary material for lamp spectrum), and a cooling fan was used to offset the irradiation-induced warming. When irradiation was applied, the actual sample temperature ranged from 24.5 to 31.8 °C, with a mean of 28.3 °C. The 4 and 40 °C incubated samples were warmed up or cooled down in a 25 °C water bath for 15 min before haloform quantification.

A CTC Combi PAL autosampler coupled with a GC-ECD (Agilent 7890) was used to analyse the haloform formation in the headspace vials. The sample vials were heated to 40 °C for 10 min in a shaker, and 1 mL of vial headspace was injected into the GC-ECD. The column was a 0.25-mm internal diameter × 30-m fused silica capillary with a chemically bonded methyl polysiloxane phase (DB-1, J&W, Agilent Technologies). The temperatures of the injection port and detector were 200 and 290 °C respectively. The GC oven temperature program was set to remain at 35 °C for 22 min, increase to 145 °C at a rate of 10 °C min^{-1}, hold at 145 °C for 2 min, and then increase to 270 °C at 20 °C min^{-1}, and then hold for 20 min.

Results

In situ emissions

Flux chamber measurements in the freshwater wetland (Site 1), oligohaline wetland (Site 2) and mesohaline saltmarsh (Site 3) showed striking differences in chloroform emissions along the salinity gradient of North Winyah Bay. As shown in Fig. 2a, the largest $CHCl_3$ emission (209 ± 183 nmol m^{-2} day^{-1}; mean ± standard deviation, $n = 4$) was observed in the degraded oligohaline wetland, compared with the mesohaline saltmarsh (71.9 ± 33.4 nmol m^{-2} day^{-1}) and freshwater wetland (9.69 ± 3.88 nmol m^{-2} day^{-1}). Although bromoform was not quantitatively measured, the largest peaks were noticed from the salt marsh flux chamber sites, which included both standing water and cordgrass vegetation. This is consistent with the aquatic experiments (*Aqueous haloform production* section) as well as other studies[62,63] that suggested that bromoform is a major haloform species produced in natural seawaters.

Soil core incubation emissions

As shown in Fig. 2b, the incubation of intact live soil cores from Sites 1 to 3 also showed the largest mean of $CHCl_3$ emissions
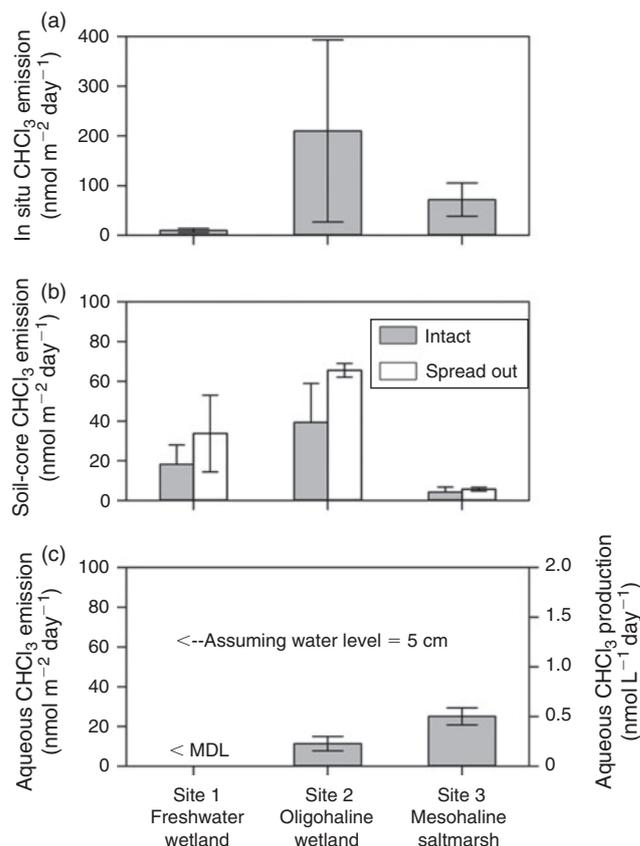

Fig. 2. $CHCl_3$ emissions from (a) in situ flux chambers in May 2012, (b) soil-core incubations and (c) aqueous incubations, from the freshwater wetland (Site 1); oligohaline wetland (Site 2); and mesohaline saltmarsh (Site 3). The aqueous $CHCl_3$ emissions based on 5-cm water level were estimated by multiplying the aqueous $CHCl_3$ production in moles per litre per day by 1000 L m^{-3} and 0.05 m (water level). The error bar represents standard deviation. (MDL, method detection limit.)

from the oligohaline wetland (39.4 ± 19.5 nmol m^{-2} day^{-1}; range: 16.2–76.4 nmol m^{-2} day^{-1}), compared with the freshwater wetland (18.3 ± 9.7 nmol m^{-2} day^{-1}) and mesohaline saltmarsh (4.32 ± 2.55 nmol m^{-2} day^{-1}). Spreading out the soil samples from the soil core on the bottom of the Mason jar (2.48 times greater soil surface area than the intact soil core) significantly increased the emissions to 1.54 ± 0.49 (range: 0.85–2.01) more than the intact soil core. Interestingly, for both intact and spread-out soils, the dead soils and live soils had no statistical difference in $CHCl_3$ emission ($P > 0.05$; paired-t-test; Fig. 3).

Aqueous haloform production

As shown in Fig. 2c, laboratory incubation of the untreated wetland waters (unfiltered and no chemical addition) indicated that the highest aqueous $CHCl_3$ production was in mesohaline saltmarsh (502 ± 86 pmol L^{-1} day^{-1}), followed by oligohaline wetland (226 ± 72 pmol L^{-1} day^{-1}). However, no detectable net $CHCl_3$ production was found in freshwater wetland or euhaline saltmarsh (<42 pmol L^{-1} day^{-1}). For $CHBr_3$, although the net increase of peak area from the ECD in the 24-h incubation appeared to follow the order of freshwater wetland < oligohaline wetland < mesohaline saltmarsh < euhaline saltmarsh, none of them were above quantifiable detection limits (all <19 pmol L^{-1} day^{-1}). Based on the production results, when the water level equals 5.0 cm, the aqueous $CHCl_3$ emissions follow the
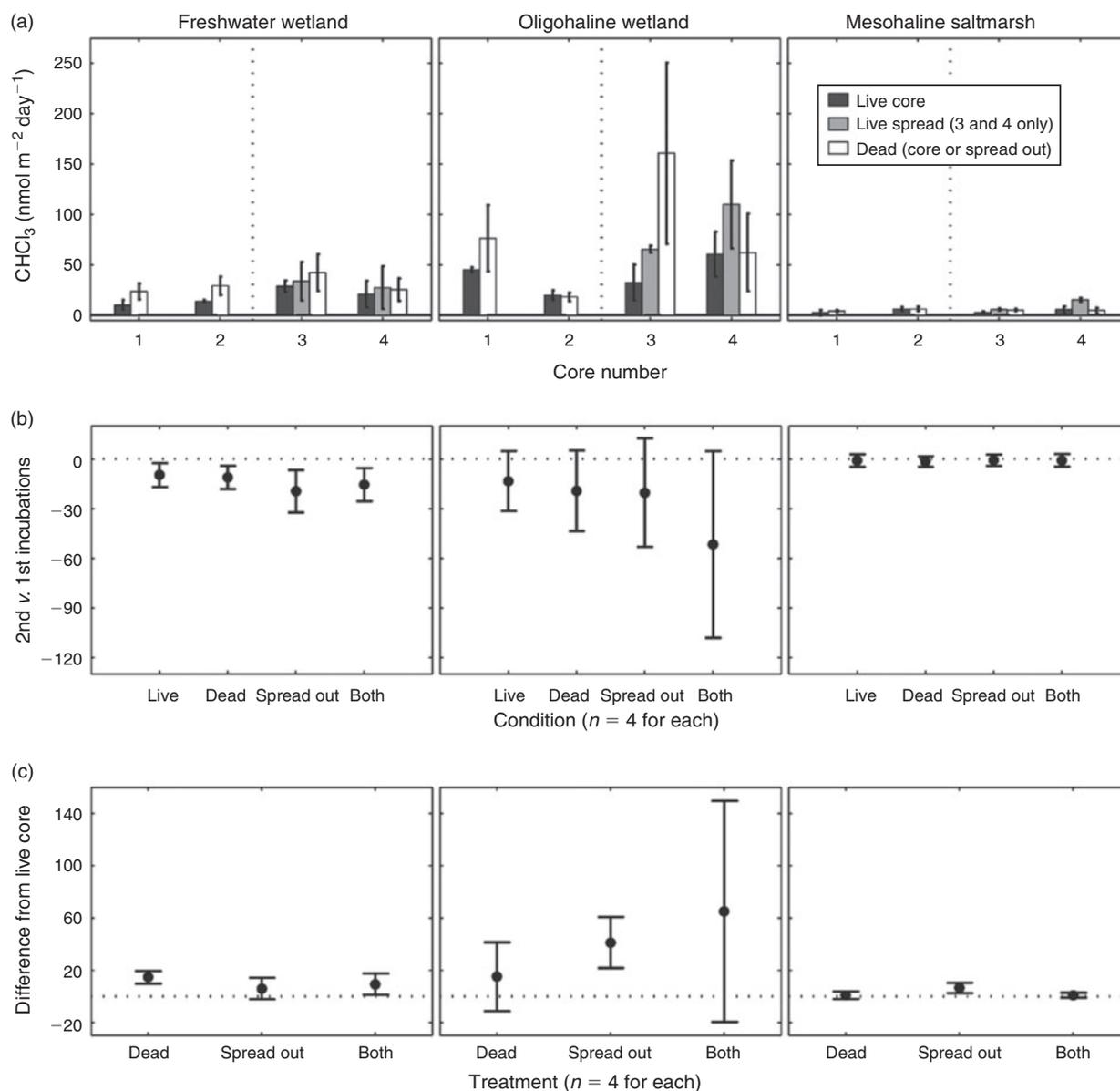
Fig. 3. (a) Chloroform emissions from the incubation of soil cores from the freshwater wetland (Site 1); oligohaline wetland (Site 2); and mesohaline saltmarsh (Site 3). (b) Effect of incubation order, quantified as a difference in flux (nmol m^{-2} day^{-1}) between the second and first incubation for each treatment type. (c) Effect of treatment (sterilisation, spreading out or both), quantified as a difference in flux (nmol m^{-2} day^{-1}) between the treated soil and the corresponding live soil-core incubation. The error bar represents standard deviation.

order: freshwater wetland or euhaline saltmarsh (<2.1 nmol m^{-2} day^{-1}) $<$ oligohaline wetland (11.3 ± 3.6 nmol m^{-2} day^{-1}) $<$ mesohaline saltmarsh (25.1 ± 4.3 nmol m^{-2} day^{-1}).

Factors affecting radical-based abiotic haloform formation

DOM characterisation

Comparison of water quality among sites indicated that the highest DOC concentrations, C/N ratio, SUVA (surrogate for DOM aromaticity), HIX (surrogate for humification degree of DOM) and lower E2/E3 (surrogate for quantum yields in singlet oxygen under sunlight irradiation) were found in waters from forest sites, compared with the saltmarsh sites for both natural and managed wetlands (Table 1, and Figs S2 and S3 in Supplementary material). In the managed wetlands, the waters in outlets consistently showed higher SUVA and HIX but a lower redox index compared with the inlets. The detailed

characteristics of the water samples are described in Table 1 and the *Characteristics of DOM* section in the Supplementary material.

Effects of water chemistry and environmental factors

Additions of H_2O_2 without Fe^{3+} (H_2O_2-only treatment) did not show net haloform production from the filtered water samples. With excess Fe^{3+} and H_2O_2 additions, production of brominated haloforms, including $CHCl_2Br$, $CHClBr_2$ and $CHBr_3$, was observed for all wetland water samples with a C : Br ratio less than 1 (Table 1). This production was observed in all oligohaline wetland, mesohaline saltmarsh, euhaline saltmarsh and managed saltwater wetland samples studied (Fig. 4). $CHBr_3$ was the major species and negligible levels of $CHCl_3$ were found in all cases. The aqueous haloform production depended on both the intrinsic water chemistry (such as halide

Table 1. Characteristics of wetland waters

All parameters were measured after filtering water through 0.45-μm filters. All values are the average of three replicates. EC_{25}, electrical conductivity at 25 °C; DOC, dissolved organic carbon; DTN, dissolved total nitrogen; [C/N] and [C/Br] are in molar ratios; SUVA, specific ultraviolet absorbance at 254 nm

	Natural forested wetlands and saltmarsh				Managed freshwater wetland		Managed saltwater wetland	
	Site 1 Freshwater wetland	Site 2 Oligohaline wetland	Site 3 Mesohaline saltmarsh	Site 4 Euhaline saltmarsh	Site 5 Inflow	Site 6 Outflow	Site 7 Inflow	Site 8 Outflow
pH	7.2	7.0	7.2	7.9	6.2	5.1	7.9	8.0
EC_{25} (mS cm^{-1})	0.27	5.45	12.0	54.3	0.22	0.16	48.1	43.3
DOC (mmol L^{-1})	2.54	2.88	0.95	0.32	4.96	5.58	0.39	0.78
DTN (μmol L^{-1})	86.9	91.7	59.1	33.9	221	333	35.6	80.8
NH_4-N (μmol L^{-1})	4.64	2.79	3.21	N.D.	13.6	27.7	9.21	10.8
NO_x-N (μmol L^{-1})	1.86	0.5	6.21	N.D.	6.93	6.36	4.93	4.36
Br$^-$ (mmol L^{-1})	N.D.	1.02	1.05	1.37	0.01	0.01	0.94	0.83
Salinity (ppt)^A	0.13	2.9	6.8	35.9	0.11	0.08	31.3	27.9
[C/N]	29.3	31.3	16.1	9.5	22.4	16.8	10.7	9.7
[C/Br]	na	2.82	0.91	0.24	992	1115	0.41	0.95
SUVA (L mg^{-1} m^{-1})	4.17	4.33	3.79	1.45	5.56	6.42	1.03	1.84
E2/E3	4.93	4.51	4.81	7.00	3.74	3.56	6.56	6.68
FI	1.41	1.39	1.46	1.47	1.30	1.31	1.48	1.54
HIX	10.3	15.6	13.4	4.18	14.0	16.7	6.47	8.65
β/α	0.51	0.49	055	0.71	0.43	0.43	0.70	0.73
Redox index	0.50	0.53	0.51	0.48	0.57	0.49	0.49	0.47

^{A}Salinity was calculated based on the practical salinity scale and is valid for surface waters with salinity between 2 and 42 ppt.[79]
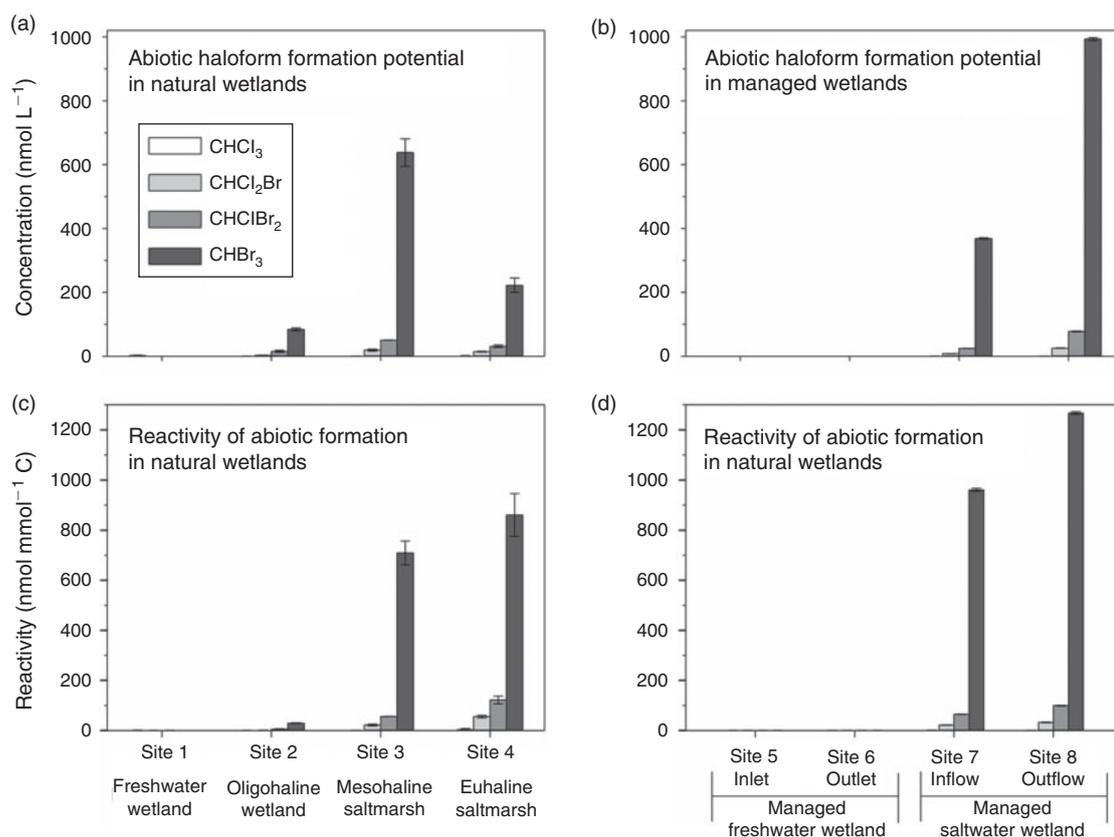

Fig. 4. Haloform formation from Fenton oxidation of waters along the salinity gradient in natural and managed wetlands. The error bar represents standard deviation.

availability and DOM source) and extrinsic environmental factors (temperature and sunlight availability).

Specifically, no haloform production was observed in either natural or managed freshwater wetland water samples that had low EC_{25} (<0.3 mS cm^{-1}; low halide availability), even with excess doses of Fenton-like reagents. With addition of 0.05 g NaCl, which is equivalent to 5 ppt salinity in the reaction vials, elevated haloform production was observed in freshwater
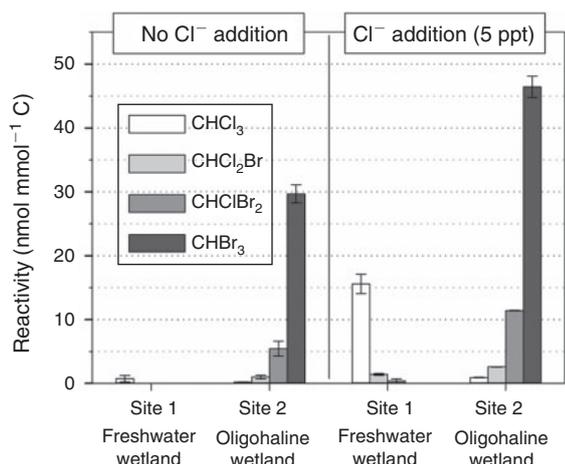
Fig. 5. Effects of chloride on the abiotic formation of haloform from freshwater (Site 1) and oligohaline (Site 2) wetland waters. The error bar represents standard deviation.

Fig. 6. Reactivity of haloform from mesohaline saltmarsh waters (Site 3) through Fenton-like reactions under different temperature and light treatments. Embedded figure shows the data in linear scale. The error bar represents standard deviation.

wetland and oligohaline wetland waters (Fig. 5) but not for mesohaline and euhaline wetland waters, which had abundant halide (no halide limitation; Fig. S4 in Supplementary material). Apparently, halide availability was the limiting factor in aqueous haloform production in the freshwater wetland. However, haloform production was not simply proportional to the EC_{25} or bromide level of water across all samples (Fig. 4). Waters from euhaline saltmarsh had the highest bromide level in water (1.37 mmol L^{-1}) but the highest $CHBr_3$ formation was observed in the outflow of the managed saltwater wetland (bromide level $= 0.83$ mmol L^{-1}). This coincided with the highest reactivity of DOC in forming $CHBr_3$ (i.e. reactivity $=$ concentration of haloform species normalised with respect to initial DOC concentration) in the outflow of the managed saltwater wetland, with an average of 1.27 μmol $CHBr_3$ $mmol^{-1}$ C. The greater formation and reactivity of haloform in the outflow (HIX $= 8.65$; SUVA $= 1.84$ L mg^{-1} m^{-1}) than the inflow (HIX $= 6.47$; SUVA $= 1.03$ L mg^{-1} m^{-1}) waters highlighted that humification increased the reactivity of DOM in abiotic haloform formation.

As shown in Fig. 6, haloform production generally increased with incubation temperature. The reactivity in bromoform formation was 263 nmol $mmol^{-1}$ C at 4 °C, increased to 1.42 μmol $mmol^{-1}$ C at 25 °C, and reached 3.70 μmol $mmol^{-1}$ C at 40 °C. Because the experiments were conducted under the same conditions except for incubation temperature, the reactivity can be considered as the reaction rate (k) at different temperatures (T). By substituting into Arrhenius' equation:

$$\ln(k) = -E_a/R(1/T) + \ln(A)$$

where A is the pre-exponential factor, E_a is the activation energy, and R is the universal gas constant), we find that ln (k) $= -6394$ $(1/T) + 14.8$ with $R^2 = 0.999$. Because the slope of the linear regression (E_a/R) is 6394, the activation energy E_a for bromoform formation was estimated to be 53.1 kJ mol^{-1}. Furthermore, light irradiation on water with Fenton reagents had an even greater effect than temperature on the halogenation processes. A 10-fold increase in reactivity of bromoform formation to 12.8 μmol $mmol^{-1}$ C was observed in the light-irradiated treatment compared with that incubated under dark conditions at 25 °C (Fig. 6). Importantly, a significant decrease in DOC concentration was observed in the light treatment (Fig. S5 in Supplementary
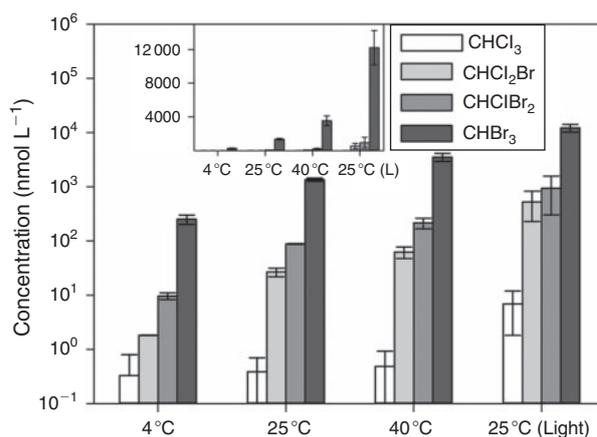
material), probably due to the photo-irradiation-enhanced Fe^{III}–Fe^{II} cycling and coagulation with DOM in water.[64,65]

Discussion

In situ, soil, and water emissions

The in situ and laboratory incubations suggest that the forest–saltmarsh transition zone (i.e. oligohaline wetland and mesohaline saltmarsh) is a hotspot of haloform production where saltwater and terrestrial DOM mix. The in situ $CHCl_3$ emission of 209 ± 183 nmol m^{-2} day^{-1} (range: 77–453 nmol m^{-2} day^{-1}) in the degraded oligohaline wetland is at the high end of common emission ranges worldwide, compared with many known $CHCl_3$ sources such as salt marshes in Tasmania, Australia (mean $= 14.7$ nmol m^{-2} day^{-1}),[16] inland and coastal marshes in Ireland (105 nmol m^{-2} day^{-1}),[14] coastal salt marshes in southern California (15 nmol m^{-2} day^{-1}),[66] peat soils at the Sacramento–San Joaquin delta in California (258 nmol m^{-2} day^{-1}),[52] and the Alaskan Arctic tundra (45 nmol m^{-2} day^{-1}).[12]

Comparison of the in situ, soil and water emissions (Fig. 2) clearly indicates that both wetlands soil and water could produce haloforms and their relative contributions to the total emissions are site-dependent. In the freshwater wetland, almost all emissions were contributed by the soil or sediment instead of water. The lack of halide in the wetland water is likely the limiting factor for aqueous $CHCl_3$ production. In the oligohaline wetland, the highest soil $CHCl_3$ emissions can explain the highest in situ $CHCl_3$ emissions across three sites. Also, aqueous production cannot be ignored in the oligohaline wetland as it reached 226 ± 72 pmol L^{-1} day^{-1}. In the mesohaline saltmarsh that receives waters from the oligohaline wetland, the aqueous $CHCl_3$ production was the highest among sites and contributed an even higher fraction of the overall in situ $CHCl_3$ emissions compared with soil emissions. These results suggest that $CHCl_3$ emission appears to be maximised in the forest–marsh transition zone where chloride is introduced into forest ecosystems with high carbon levels, as evidenced by the largest emissions at the oligohaline wetland flux chambers.

Significance of abiotic haloform formation

Using a sterilisation approach, the $CHCl_3$ emissions from live and dead soil cores were compared but no significant difference

was found (Fig. 3c). This result suggests that the abiotic process is likely an important process in soil $CHCl_3$ production in coastal wetlands. It appeared to be different from previous studies that indicated predominantly biotic halomethanes production over abiotic production at a coniferous forest within the Stubbetorp catchment in south-eastern Sweden[67] or hypersaline sediments of Lake Strawbridge and Lake Orr in Western Australia.[68,69] Abundant ferric and ferrous ions from shallow groundwater of the wetlands[70–72] may facilitate the abiotic halogenation process of $CHCl_3$. However, the detailed abiotic formation mechanism in soil remains unclear and future studies on reaction mechanisms will elucidate the chemical reactions in the soil cores. It is not known if the heating process ($\sim$90 °C) leads to complete sterilisation or generates precursors of $CHCl_3$ that remained 24 h later when incubations began. However, this sterilisation method has been shown to eliminate the biologically mediated methyl halide uptake by soils.[53] Current sterilisation approaches cannot completely inhibit enzymatic reactivity without changing soil organic matter[73]; however, comparing different sterilisation approaches in the future will help to more accurately understand abiotic v. biotic haloform formation.

With the addition of Fenton-like reagents, the high levels of radical-based haloform production in wetland waters indicate the possibility of abiotic haloform formation from surface water. Thermodynamic redox calculations also indicated that radical-based haloform production by formation of hydroxyl radical and HOX is thermodynamically favoured.[74] Also, in the presence of bromide, reactive bromine species are more energetically favoured to be formed than reactive chlorine species for the same oxidation coupling reaction. The radical-based halogenation also transforms bromide rapidly to the reactive bromine species with high reaction rate constants.[75] Therefore, $CHBr_3$ becomes the major species of haloform as the reactive bromine species react with DOM in the radical-based halogenation tests.[19,75]

The present study clearly indicates that halide availability, organic matter chemistry, temperature and light irradiation can affect haloform formation by radical-based halogenation. Halide availability was found to be a major limiting factor in freshwater wetlands. DOM has been previously found to affect the yield of haloform by enzymatic halogenation,[32,33] and the present study suggests that DOM chemistry is also important in affecting the yield of haloform by radical halogenation. Particularly, DOM with a higher aromaticity or humification degree from the outlet of managed saltmarsh wetland showed the highest reactivity in haloform formation. In addition to the effects of water chemistry, light irradiation is a key factor to promote radical-based halogenation and high temperature also favours haloform production.

Environmental implication

Because the tidal freshwater forests and marshes are common landscapes in the south-eastern US, covering >200 000 ha,[37] the forest–marsh transition zones are likely to have contributed high haloform emissions to the atmosphere. Sea-level rise and seawater intrusion have posed threats to the freshwater forest wetland and have been gradually changing the freshwater forest wetland to degraded oligohaline wetland. As the degraded oligohaline wetland has showed strikingly higher overall in situ, soil and aqueous $CHCl_3$ emissions compared with the freshwater wetland, sea-level rise and seawater intrusion, which introduce halide and potentially halogenating enzymes, are expected to largely increase the $CHCl_3$ emission from the

affected and gradually degraded freshwater wetlands. Specifically, the predominant haloform source shifts from sediment emission to water emission from freshwater wetland to mesohaline saltmarsh. Whereas the freshwater wetland presents soil-dominated haloform production and mesohaline saltmarsh shows tidal-water-dominated haloform production, the degraded oligohaline wetland in the transition zone appears to combine both favourable conditions of terrestrial and marine productions and becomes the largest emission source.

For the global haloform budget, it has been proposed that offshore seawater and soil processes are both important $CHCl_3$ sources,[8] whereas coastal seawater and the open ocean are major $CHBr_3$ sources.[76,77] Although we found high emissions from degraded oligohaline wetlands in the present study, we are still far from the actual quantification of haloform emission from such a landscape regionally or globally. Long-term and more intensive monitoring of the haloform fluxes and exploration of the formation mechanisms in degrading wetland ecosystems will help clarify how sea-level rise can potentially change the global haloform budget.

Some results of the current study also have implications on the future optimisation of methodology in haloform flux quantification. For example, the elevated $CHCl_3$ emission from spread-out soil cores compared with intact soil cores suggested that soil pores can store a significant fraction of $CHCl_3$. Therefore, for the in situ measurement of haloform fluxes in coastal wetlands, attention is needed to minimise the potential human or animal effects on squeezing out haloform from the wetland soil or sediment pores, particularly for the high-emission sites. Also, based on previous studies[19,78] and the present study, abiotic haloform formation is actually happening in both soil and water samples and highly sensitive to site-specific halide availability, organic matter chemistry and environmental factors. In particular, light irradiation is a critical factor on increasing the radical-based abiotic haloform production by one order of magnitude. However, many in situ chamber studies use non-transparent materials, which may cause underestimation of the actual haloform emission from the coastal wetlands by excluding the effect of sunlight. Future studies comparing clear and opaque chambers will help to better understand the effect of sunlight on halocarbon emissions in coastal ecosystems.

References

[1] *Scientific Assessment of Ozone Depletion: 2014. World Meteorological Organization. Global Ozone Research and Monitoring Project – Report number 55* **2014** (World Meteorological Organization: Geneva, Switzerland).

[2] S. Montzka, S. Reimann, D. Blake, M. Dorf, A. Engel, P. Fraser, L. Froidevaux, K. Jucks, K. Kreher, K. Krüger, Ozone-depleting

substances (ODSs) and related chemicals, in *Scientific Assessment of Ozone Depletion: 2010, Global Ozone Research and Monitoring Project – Report number 52* **2011**, Ch. 5, pp. 1–108 (World Meteorological Organization: Geneva, Switzerland).

[3] R. Hossaini, M. Chipperfield, A. Saiz-Lopez, J. Harrison, R. Glasow, R. Sommariva, E. Atlas, M. Navarro, S. Montzka, W. Feng, Growth in stratospheric chlorine from short-lived chemicals not controlled by the Montreal Protocol. *Geophys. Res. Lett.* **2015**, *42*, 4573. doi:10.1002/2015GL063783

[4] J. J. Rook, Formation of haloforms during chlorination of natural waters. *J. Water Treat. Exam.* **1974**, *23*, 234.

[5] S. D. Richardson, M. J. Plewa, E. D. Wagner, R. Schoeny, D. M. DeMarini, Occurrence, genotoxicity, and carcinogenicity of regulated and emerging disinfection by-products in drinking water: a review and roadmap for research. *Mutat. Res. Rev. Mutat. Res.* **2007**, *636*, 178. doi:10.1016/J.MRREV.2007.09.001

[6] J. J. Wang, A. T. Chow, J. M. Sweeney, J. A. Mazet, Trihalomethanes in marine mammal aquaria: occurrences, sources, and health risks. *Water Res.* **2014**, *59*, 219. doi:10.1016/J.WATRES.2014.04.007

[7] F. Laturnus, K. F. Haselmann, T. Borch, C. Gron, Terrestrial natural sources of trichloromethane (chloroform, $CHCl_3$) – an overview. *Biogeochemistry* **2002**, *60*, 121. doi:10.1023/A:1019887505651

[8] A. McCulloch, Chloroform in the environment: occurrence, sources, sinks and effects. *Chemosphere* **2003**, *50*, 1291. doi:10.1016/S0045-6535(02)00697-5

[9] D. R. Worton, W. T. Sturges, J. Schwander, R. Mulvaney, J. M. Barnola, J. Chappellaz, 20th century trends and budget implications of chloroform and related tri- and dihalomethanes inferred from firn air. *Atmos. Chem. Phys.* **2006**, *6*, 2847. doi:10.5194/ACP-6-2847-2006

[10] L. J. Carpenter, P. S. Liss, On temperate sources of bromoform and other reactive organic bromine gases. *J. Geophys. Res. Atmos.* **2000**, *105*, 20539. doi:10.1029/2000JD900242

[11] H.-F. Schöler, W. Thiemann, Natural formation of trihalomethanes in the marine and terrestrial environment. *GDCh Monograph* **2005**, *34*, 122.

[12] R. C. Rhew, Y. A. Teh, T. Abel, A. Atwood, O. Mazeas, Chloroform emissions from the Alaskan Arctic tundra. *Geophys. Res. Lett.* **2008**, *35*, L21811. doi:10.1029/2008GL035762

[13] R. C. Rhew, B. R. Miller, R. F. Weiss, Chloroform, carbon tetrachloride and methyl chloroform fluxes in southern California ecosystems. *Atmos. Environ.* **2008**, *42*, 7135. doi:10.1016/J.ATMOSENV.2008.05.038

[14] C. H. Dimmer, P. G. Simmonds, G. Nickless, M. R. Bassford, Biogenic fluxes of halomethanes from Irish peatland ecosystems. *Atmos. Environ.* **2001**, *35*, 321. doi:10.1016/S1352-2310(00)00151-5

[15] E. J. Hoekstra, E. W. B. De Leer, U. A. T. Brinkman, Natural formation of chloroform and brominated trihalomethanes in soil. *Environ. Sci. Technol.* **1998**, *32*, 3724. doi:10.1021/ES980127C

[16] M. L. Cox, P. J. Fraser, G. A. Sturrock, S. T. Siems, L. W. Porter, Terrestrial sources and sinks of halomethanes near Cape Grim, Tasmania. *Atmos. Environ.* **2004**, *38*, 3839. doi:10.1016/J.ATMOSENV.2004.03.050

[17] C. N. Albers, O. S. Jacobsen, E. M. M. Flores, J. S. F. Pereira, T. Laier, Spatial variation in natural formation of chloroform in the soils of four coniferous forests. *Biogeochemistry* **2011**, *103*, 317. doi:10.1007/S10533-010-9467-9

[18] M. A. K. Khalil, R. A. Rasmussen, M. X. Wang, L. Ren, Emissions of trace gases from Chinese rice fields and biogas generators – CH_4, N_2O, CO, CO_2, chlorocarbons, and hydrocarbons. *Chemosphere* **1990**, *20*, 207. doi:10.1016/0045-6535(90)90097-D

[19] S. G. Huber, K. Kotte, H. F. Scholer, J. Williams, Natural abiotic formation of trihalomethanes in soil: results from laboratory studies and field samples. *Environ. Sci. Technol.* **2009**, *43*, 4934. doi:10.1021/ES8032605

[20] J. J. Wang, T. W. Ng, Q. Zhang, X. B. Yang, R. A. Dahlgren, A. T. Chow, P. K. Wong, Technical note: reactivity of C1 and C2 organohalogens formation – from plant litter to bacteria. *Biogeosciences* **2012**, *9*, 3721. doi:10.5194/BG-9-3721-2012

[21] K. Ballschmiter, Pattern and sources of naturally produced organohalogens in the marine environment: biogenic formation of organohalogens. *Chemosphere* **2003**, *52*, 313. doi:10.1016/S0045-6535(03)00211-X

[22] C. Paul, G. Pohnert, Production and role of volatile halogenated compounds from marine algae. *Nat. Prod. Rep.* **2011**, *28*, 186. doi:10.1039/C0NP00043D

[23] F. Laturnus, I. Fahimi, M. Gryndler, A. Hartmann, M. R. Heal, M. Matucha, H. F. Scholer, R. Schroll, T. Svensson, Natural formation and degradation of chloroacetic acids and volatile organochlorines in forest soil – challenges to understanding. *Environ. Sci. Pollut. Res.* **2005**, *12*, 233. doi:10.1065/ESPR2005.06.262

[24] I. J. Fahimi, F. Keppler, H. F. Scholer, Formation of chloroacetic acids from soil, humic acid and phenolic moieties. *Chemosphere* **2003**, *52*, 513. doi:10.1016/S0045-6535(03)00212-1

[25] G. Öberg, The natural chlorine cycle – fitting the scattered pieces. *Appl. Microbiol. Biotechnol.* **2002**, *58*, 565. doi:10.1007/S00253-001-0895-2

[26] G. W. Gribble, *Naturally Occurring Organohalogen Compounds – A Comprehensive Update* **2010** (Springer Verlag: Vienna, Austria).

[27] A. Butler, M. Sandy, Mechanistic considerations of halogenating enzymes. *Nature* **2009**, *460*, 848. doi:10.1038/NATURE08303

[28] C. Wagner, M. El Omari, G. M. Konig, Biohalogenation: nature's way to synthesize halogenated metabolites. *J. Nat. Prod.* **2009**, *72*, 540. doi:10.1021/NP800651M

[29] S. C. B. Myneni, Formation of stable chlorinated hydrocarbons in weathering plant material. *Science* **2002**, *295*, 1039. doi:10.1126/SCIENCE.1067153

[30] A. T. Chow, R. A. Dahlgren, J. A. Harrison, Watershed sources of disinfection byproduct precursors in the Sacramento and San Joaquin rivers, California. *Environ. Sci. Technol.* **2007**, *41*, 7645. doi:10.1021/ES070621T

[31] M. Gustavsson, S. Karlsson, G. Oberg, P. Sanden, T. Svensson, S. Valinia, Y. Thiry, D. Bastviken, Organic matter chlorination rates in different boreal soils: the role of soil organic matter content. *Environ. Sci. Technol.* **2012**, *46*, 1504. doi:10.1021/ES203191R

[32] Y. N. Liu, D. C. O. Thornton, T. S. Bianchi, W. A. Arnold, M. R. Shields, J. Chen, S. A. Yvon-Lewis, Dissolved organic matter composition drives the marine production of brominated very short-lived substances. *Environ. Sci. Technol.* **2015**, *49*, 3366. doi:10.1021/ES505464K

[33] C. Y. Lin, S. L. Manley, Bromoform production from seawater treated with bromoperoxidase. *Limnol. Oceanogr.* **2012**, *57*, 1857. doi:10.4319/LO.2012.57.6.1857

[34] P. Bengtson, D. Bastviken, W. de Boer, G. Oberg, Possible role of reactive chlorine in microbial antagonism and organic matter chlorination in terrestrial environments. *Environ. Microbiol.* **2009**, *11*, 1330. doi:10.1111/J.1462-2920.2009.01915.X

[35] J. D. Méndez-Díaz, K. K. Shimabuku, J. Ma, Z. O. Enumah, J. J. Pignatello, W. A. Mitch, M. C. Dodd, Sunlight-driven photochemical halogenation of dissolved organic matter in seawater: a natural abiotic source of organobromine and organoiodine. *Environ. Sci. Technol.* **2014**, *48*, 7418. doi:10.1021/ES5016668

[36] V. R. Burkett, D. B. Zilkoski, D. A. Hart, Sea-level rise and subsidence: Implications for flooding in New Orleans, Louisiana in *US Geological Survey Subsidence Interest Group Conference: Proceedings of the Technical Meeting*, 27–29 November 2001, Galveston, TX, **2002**, pp. 63–70 (US Geological Survey: Galveston, TX).

[37] D. W. Field, A. J. Reyer, P. V. Genovese, B. D. Shearer, *Coastal Wetlands of the United States: an Accounting of a Valuable National Resource: a Special NOAA 20th Anniversary Report* **1991** (NOAA: Washington, DC).

[38] W. H. Conner, T. W. Doyle, K. W. Krauss, *Ecology of Tidal Freshwater Forested Wetlands of the South-Eastern United States* **2007** (Springer: New York).

[39] J. T. Morris, P. V. Sundareshwar, C. T. Nietch, B. Kjerfve, D. R. Cahoon, Responses of coastal wetlands to rising sea level. *Ecology* **2002**, *83*, 2869. doi:10.1890/0012-9658(2002)083[2869:ROCWTR]2.0.CO;2

[40] N. Cormier, K. W. Krauss, W. H. Conner, Periodicity in stem growth and litterfall in tidal freshwater forested wetlands: influence of salinity and drought on nitrogen recycling. *Estuaries Coasts* **2013**, *36*, 533. doi:10.1007/S12237-012-9505-Z

[41] M. A. Goñi, K. A. Thomas, Sources and transformations of organic matter in surface soils and sediments from a tidal estuary (north inlet, South Carolina, USA). *Estuaries* **2000**, *23*, 548. doi:10.2307/1353145

[42] T. Williams, A. T. Chow, B. Song, Historical visualization evidence on forest–salt marsh transition in Winyah Bay, South Carolina: a retrospective study in sea level rise. *Wetland Sci. Prac.* **2012**, *29*, 5.

[43] A. T. Chow, D. M. Leech, T. H. Boyer, P. C. Singer, Impact of simulated solar irradiation on disinfection byproduct precursors. *Environ. Sci. Technol.* **2008**, *42*, 5586. doi:10.1021/ES800206H

[44] N. M. Scully, D. J. McQueen, D. R. S. Lean, W. J. Cooper, Hydrogen peroxide formation: the interaction of ultraviolet radiation and dissolved organic carbon in lake waters along a 43–75°N gradient. *Limnol. Oceanogr.* **1996**, *41*, 540. doi:10.4319/LO.1996.41.3.0540

[45] W. J. Cooper, R. G. Zika, R. G. Petasne, J. M. C. Plane, Photochemical formation of H_2O_2 in natural waters exposed to sunlight. *Environ. Sci. Technol.* **1988**, *22*, 1156. doi:10.1021/ES00175A004

[46] D. Vione, G. Falletti, V. Maurino, C. Minero, E. Pelizzetti, M. Malandrino, R. Ajassa, R. I. Olariu, C. Arsene, Sources and sinks of hydroxyl radicals upon irradiation of natural water samples. *Environ. Sci. Technol.* **2006**, *40*, 3775. doi:10.1021/ES052206B

[47] A. T. Chow, J. N. Dai, W. H. Conner, D. R. Hitchcock, J. J. Wang, Dissolved organic matter and nutrient dynamics of a coastal freshwater forested wetland in Winyah Bay, South Carolina. *Biogeochemistry* **2013**, *112*, 571. doi:10.1007/S10533-012-9750-Z

[48] K. W. Krauss, J. A. Duberstein, T. W. Doyle, W. H. Conner, R. H. Day, L. W. Inabinette, J. L. Whitbeck, Site condition, structure, and growth of baldcypress along tidal/non-tidal salinity gradients. *Wetlands* **2009**, *29*, 505. doi:10.1672/08-77.1

[49] J. N. Dai, J. J. Wang, A. T. Chow, W. H. Conner, Electrical energy production from forest detritus in a forested wetland using microbial fuel cells. *Glob. Change Biol. Bioenergy* **2015**, *7*, 244. doi:10.1111/GCBB.12117

[50] K. W. Krauss, J. L. Whitbeck, Soil greenhouse gas fluxes during wetland forest retreat along the lower Savannah River, Georgia (USA). *Wetlands* **2012**, *32*, 73. doi:10.1007/S13157-011-0246-8

[51] M. A. H. Khan, R. C. Rhew, M. E. Whelan, K. Zhou, S. Deverel, Methyl halide and chloroform emissions from a subsiding Sacramento–San Joaquin delta island converted to rice fields. *Atmos. Environ.* **2011**, *45*, 977. doi:10.1016/J.ATMOSENV.2010.10.053

[52] M. A. H. Khan, M. E. Whelan, R. C. Rhew, Effects of temperature and soil moisture on methyl halide and chloroform fluxes from drained peatland pasture soils. *J. Environ. Monit.* **2012**, *14*, 241. doi:10.1039/C1EM10639B

[53] R. C. Rhew, M. Aydin, E. S. Saltzman, Measuring terrestrial fluxes of methyl chloride and methyl bromide using a stable isotope tracer technique. *Geophys. Res. Lett.* **2003**, *30*, 2103. doi:10.1029/2003GL018160

[54] M. Neal, C. Neal, H. Wickham, S. Harman, Determination of bromide, chloride, fluoride, nitrate and sulphate by ion chromatography: comparisons of methodologies for rainfall, cloud water and river waters at the Plynlimon catchments of mid-Wales. *Hydrol. Earth Syst. Sci.* **2007**, *11*, 294. doi:10.5194/HESS-11-294-2007

[55] A. D. Eaton, M. A. H. Franson, *Standard Methods for the Examination of Water & Wastewater* **2005** (American Public Health Association: Washington, DC).

[56] J. L. Weishaar, G. R. Aiken, B. A. Bergamaschi, M. S. Fram, R. Fujii, K. Mopper, Evaluation of specific ultraviolet absorbance as an indicator of the chemical composition and reactivity of dissolved organic carbon. *Environ. Sci. Technol.* **2003**, *37*, 4702. doi:10.1021/ES030360X

[57] J. Peuravuori, K. Pihlaja, Molecular size distribution and spectroscopic properties of aquatic humic substances. *Anal. Chim. Acta* **1997**, *337*, 133. doi:10.1016/S0003-2670(96)00412-6

[58] R. M. Dalrymple, A. K. Carfagno, C. M. Sharpless, Correlations between dissolved organic matter optical properties and quantum yields of singlet oxygen and hydrogen peroxide. *Environ. Sci. Technol.* **2010**, *44*, 5824. doi:10.1021/ES101005U

[59] K. R. Murphy, K. D. Butler, R. G. M. Spencer, C. A. Stedmon, J. R. Boehme, G. R. Aiken, Measurement of dissolved organic matter fluorescence in aquatic environments: an interlaboratory comparison. *Environ. Sci. Technol.* **2010**, *44*, 9405. doi:10.1021/ES102362T

[60] J. B. Fellman, E. Hood, R. G. M. Spencer, Fluorescence spectroscopy opens new windows into dissolved organic matter dynamics in freshwater ecosystems: a review. *Limnol. Oceanogr.* **2010**, *55*, 2452. doi:10.4319/LO.2010.55.6.2452

[61] R. M. Cory, D. M. McKnight, Fluorescence spectroscopy reveals ubiquitous presence of oxidized and reduced quinones in dissolved organic matter. *Environ. Sci. Technol.* **2005**, *39*, 8142. doi:10.1021/ES0506962

[62] C. Hughes, A. L. Chuck, H. Rossetti, P. J. Mann, S. M. Turner, A. Clarke, R. Chance, P. S. Liss, Seasonal cycle of seawater bromoform and dibromomethane concentrations in a coastal bay on the western Antarctic Peninsula. *Global Biogeochem. Cycles* **2009**, *23*, GB2024. doi:10.1029/2008GB003268

[63] Y. N. Liu, S. A. Yvon-Lewis, L. Hu, J. E. Salisbury, J. E. O'Hern, $CHBr_3$, CH_2Br_2, and $CHClBr_2$ in US coastal waters during the Gulf of Mexico and East Coast Carbon cruise. *J. Geophys. Res. – Oceans* **2011**, *116*, C10004. doi:10.1029/2010JC006729

[64] M. Fujii, A. L. Rose, T. D. Waite, T. Omura, Oxygen and superoxide-mediated redox kinetics of iron complexed by humic substances in coastal seawater. *Environ. Sci. Technol.* **2010**, *44*, 9337. doi:10.1021/ES102583C

[65] M. P. Miller, D. M. McKnight, S. C. Chapra, Production of microbially derived fulvic acid from photolysis of quinone-containing extracellular products of phytoplankton. *Aquat. Sci.* **2009**, *71*, 170. doi:10.1007/S00027-009-9194-2

[66] R. C. Rhew, Sources and sinks of methyl bromide and methyl chloride in the tallgrass prairie: applying a stable isotope tracer technique over highly variable gross fluxes. *J. Geophys. Res. Biogeosci.* **2011**, *116*, G03026. doi:10.1029/2011JG001704

[67] D. Bastviken, T. Svensson, S. Karlsson, P. Sanden, G. Oberg, Temperature sensitivity indicates that chlorination of organic matter in forest soil is primarily biotic. *Environ. Sci. Technol.* **2009**, *43*, 3569. doi:10.1021/ES8035779

[68] A. Ruecker, P. Weigold, S. Behrens, M. Jochmann, J. Laaks, A. Kappler, Predominance of biotic over abiotic formation of halogenated hydrocarbons in hypersaline sediments in Western Australia. *Environ. Sci. Technol.* **2014**, *48*, 9170. doi:10.1021/ES501810G

[69] A. Ruecker, P. Weigold, S. Behrens, M. Jochmann, X. Osorio, A. Kappler, Halogenated hydrocarbon formation in a moderately acidic salt lake in Western Australia – a role of abiotic and biotic processes. *Environ. Chem.* **2015**, *12*, 406. doi:10.1071/EN14202

[70] F. Keppler, R. Eiden, V. Niedan, J. Pracht, H. F. Scholer, Halocarbons produced by natural oxidation processes during degradation of organic matter. *Nature* **2000**, *403*, 298. doi:10.1038/35002055

[71] M. Egger, O. Rasigraf, C. J. Sapart, T. Jilbert, M. S. M. Jetten, T. Rockmann, C. van der Veen, N. Banda, B. Kartal, K. F. Ettwig, C. P. Slomp, Iron-mediated anaerobic oxidation of methane in brackish coastal sediments. *Environ. Sci. Technol.* **2015**, *49*, 277. doi:10.1021/ES503663Z

[72] M. M. Lorah, L. D. Olsen, Natural attenuation of chlorinated volatile organic compounds in a freshwater tidal wetland: field evidence of anaerobic biodegradation. *Water Resour. Res.* **1999**, *35*, 3811. doi:10.1029/1999WR900116

[73] A. Lakzian, Evaluation of chemical and biological consequences of soil sterilization methods. *Caspian J. Env. Sci.* **2007**, *5*, 87–91.

[74] G. W. Luther III, *Thermodynamic Redox Calculations for One- and Two-Electron Transfer Steps: Implications for Halide Oxidation and Halogen Environmental Cycling* **2011** (American Chemical Society: Washington, DC).

[75] J. E. Grebel, J. J. Pignatello, W. Song, W. J. Cooper, W. A. Mitch, Impact of halides on the photobleaching of dissolved organic matter. *Mar. Chem.* **2009**, *115*, 134. doi:10.1016/J.MARCHEM. 2009.07.009

[76] I. Stemmler, I. Hense, B. Quack, Marine sources of bromoform in the global open ocean – global patterns and emissions. *Biogeosciences* **2015**, *12*, 1967. doi:10.5194/BG-12-1967-2015

[77] P. G. Simmonds, R. G. Derwent, A. J. Manning, S. O'Doherty, G. Spain, Natural chloroform emissions from the blanket peat bogs in the vicinity of Mace Head, Ireland, over a 14-year period. *Atmos. Environ.* **2010**, *44*, 1284. doi:10.1016/J.ATMOSENV.2009. 12.027

[78] F. Breider, C. N. Albers, Formation mechanisms of trichloromethyl-containing compounds in the terrestrial environment: a critical review. *Chemosphere* **2015**, *119*, 145. doi:10.1016/J.CHEMOSPHERE.2014. 05.080

[79] American Public Health Association, *Standard Methods for the Examination of Water and Wastewater (1999)*, 20th edn **1999** (American Public Health Association (APHA) and American Water Works Association: Washington, DC).